Randolph Glacier Inventory – A Dataset of Global Glacier Outlines: Version 3.2
31 Aug 2013

GLIMS Technical Report

Dataset Description

The Randolph Glacier Inventory (RGI) is a globally complete inventory of glacier outlines. It is supplemental to the Global Land Ice Measurements from Space initiative (GLIMS). Production of the RGI was motivated by the forthcoming Fifth Assessment Report of the Intergovernmental Panel on Climate Change (IPCC AR5). The RGI was released initially with little documentation in view of the IPCC's tight deadlines during 2012. More documentation is provided in the current version of this Technical Report, and the RGI itself now attaches a limited but uniform set of attributes to each glacier outline. It is intended that in due course the content of the RGI will be merged into the database of GLIMS.

Version History

Version 1.0 of the Randolph Glacier Inventory was released in February 2012. An unofficial update to Version 1.0 was provided in April 2012 to replace several regions that had topology errors and repeated polygons. Version 2.0, released in June 2012, was quality-controlled to eliminate a number of flaws, and provides a uniform set of data fields for each glacier complex. Several outlines were also improved, and a number of outlines were added in previously omitted regions. Version 2.0 also added shapefiles for its first-order and second-order regions.

Version 3.0 was an interim release representing the RGI as of 7 April 2013. It was the basis for the work of Gardner et al. (2013). The main improvements included identification of all tidewater basins, and separation of glacier complexes into glaciers in nearly all regions. Version 3.2 includes additional separation of glacier complexes into glaciers, and a repair of some geometry errors. It is the basis for the general description and analysis of the RGI presented by Pfeffer et al. (2013, submitted).

Data Distribution Policy

The Randolph Glacier Inventory has hitherto been made available under certain transitional usage constraints:

1) It is intended for the estimation of total ice volumes and glacier mass changes at global and large-regional scales;
2) It is not to be used for reporting that focuses primarily on the properties of the inventory itself, such as global size distributions, or area/elevation distributions of glaciers; and
3) It is not to be distributed.

These constraints will lapse upon the publication of the contribution of Working Group I (Physical Science) to the IPCC AR5.

Data Sources

The RGI is a combination of both new and existing published glacier outlines. New outlines were provided by the glaciological community in response to requests for data on the GLIMS and Cryolist e-mail listservers. We visualized the data in a GIS by overlaying outlines on modern satellite imagery, and assessed their quality relative to other available products. In several regions the outlines already in GLIMS were used for RGI. Data from the World Glacier Inventory

(WGI, http://nsidc.org/data/docs/noaa/g01130_glacier_inventory/; WGI, 1989) and the related WGI-XF (Cogley, 2009) were used for some glaciers in the Pyrenees and in northern Asia, with outlines approximated by circles of area equaling those reported in the source. Where no other data were available we relied on data from the Digital Chart of the World (Danko, 1992).

Dataset Reference
The following reference should be used when citing RGI version 3.2:

Arendt, A., T. Bolch, J.G. Cogley, A. Gardner, J.-O. Hagen, R. Hock, G. Kaser, W.T. Pfeffer, G. Moholdt, F. Paul, V. Radić, L. Andreassen, S. Bajracharya, N. Barrand, M. Beedle, E. Berthier, R. Bhambri, A. Bliss, I. Brown, D. Burgess, E. Burgess, F. Cawkwell, T. Chinn, L. Copland, B. Davies, H. De Angelis, E. Dolgova, K. Filbert, R.R. Forester, A. Fountain, H. Frey, B. Giffen, N. Glasser, S. Gurney, W. Hagg, D. Hall, U.K. Haritashya, G. Hartmann, C. Helm, S. Herreid, I. Howat, G. Kapustin, T. Khromova, C. Kienholz, M. Köonig, J. Kohler, D. Kriegel, S. Kutuzov, I. Lavrentiev, R. Le Bris, J. Lund, W. Manley, C. Mayer, E. Miles, X. Li, B. Menounos, A. Mercer, N. Mölg, P. Mool, G. Nosenko, A. Negrete, C. Nuth, R. Pettersson, A. Racoviteanu, R. Ranzi, P. Rastner, F. Rau, B. Raup, J. Rich, H. Rott, C. Schneider, Y. Seliverstov, M. Sharp, O. Sigurðsson, C. Stokes, R. Wheate, S. Winsvold, G. Wolken, F. Wyatt, N. Zheltyhina. 2012, Randolph Glacier Inventory – A Dataset of Global Glacier Outlines: Version 3.2. Global Land Ice Measurements from Space, Boulder Colorado, USA. Digital Media.

The first 11 authors comprise an ad-hoc committee that was responsible for assembly of the RGI. The remaining authors are data contributors, listed in alphabetical order. Note that some of the 11 committee members also contributed data. Although efforts have been made to trace the names of GLIMS contributors whose outlines are now in RGI, it is possible that some have been missed. We also do not include the name of every contributor to the WGI or WGI-XF who provided information that may be incorporated in RGI. Interested users are encouraged to access the site http://glims.org/About/contributors.php for more information on GLIMS contributors, and http://nsidc.org/data/docs/noaa/g01130_glacier_inventory for more documentation on the WGI.

Region Definitions
We define 19 first-order glacier regions drawn mostly from Radić and Hock (2010), with some minor modifications (Figure 1). We further subdivide the first-order regions into second-order regions, of which there are 89 in total.
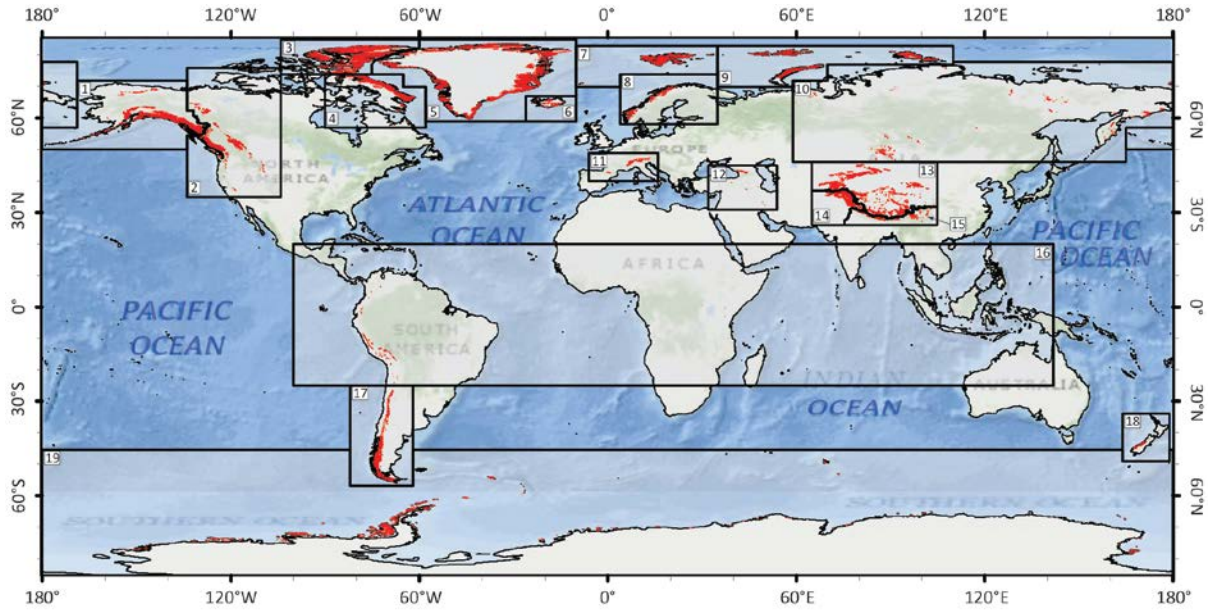
Figure 1. First-order regions of the Randolph Glacier Inventory, version 3.2.

First-order regions 01 and 10 straddle the 180th meridian, and so do second-order regions 01-03 and 19-15. For convenience of analysis in a cylindrical-equidistant coordinate system centred on longitude 0°, as in Figure 1, each of these regions appears in the accompanying shapefiles as two polygons, eastern and western.

Table 1. First-order and second-order regions of the Randolph Glacier Inventory, version 3.2.

First-order region		Second-order region (code, glacierized area in km^2, name)		
01	Alaska	01-01	346	N Alaska
		01-02	16276	Alaska Ra (Wrangell/Kilbuck)
		01-03	1913	Alaska Pena (Aleutians)
		01-04	12315	W Chugach Mtns (Talkeetna)
		01-05	33269	St Elias Mtns
		01-06	22997	N Coast Ranges
02	Western Canada and USA	02-01	128	Melville Island
		02-02	657	Mackenzie and Selwyn Mtns
		02-03	8814	S Coast Ranges
		02-04	4386	N Rocky Mtns
		02-05	468	Cascade Ra and Sa Nevada
		02-06	110	S Rocky Mtns
03	Arctic Canada (North)	03-01	27213	N Ellesmere Island
		03-02	11907	Axel Heiberg and Meighen Is
		03-03	21401	NC Ellesmere Island
		03-04	19294	SC Ellesmere Island
		03-05	10061	S Ellesmere Island (NW Devon)
		03-06	14998	Devon Island
04	Arctic Canada (South)	04-01	4874	Bylot Island
		04-02	3324	W Baffin Island
		04-03	496	N Baffin Island

		04-04	8233	NE Baffin Island
		04-05	9919	EC Baffin Island
		04-06	7944	SE Baffin Island
		04-07	5843	Cumberland Sound
		04-08	247	Frobisher Bay
		04-09	14	Labrador
05	Greenland	05-01	89794	Greenland (periphery)
		05-11	—	Greenland Ice Sheet
06	Iceland	06-00	11060	Iceland
07	Svalbard and Jan Mayen	07-01	33837	Svalbard
		07-02	121	Jan Mayen
08	Scandinavia	08-01	1490	S Norway
		08-02	1362	N Scandinavia
09	Russian Arctic	09-01	12762	Franz Josef Land
		09-02	22128	Novaya Zemlya
		09-03	16701	Severnaya Zemlya
10	North Asia	10-01	51	North Asia (North)
		10-02	1565	North Asia (East)
		10-03	17	E Chukotka[a]
		10-04	1818	Altay and Sayan
11	Central Europe	11-01	2052	Alps
		11-02	11	Pyrenees and Apennines
12	Caucasus and Middle East	12-01	1101	Greater Caucasus
		12-02	38	Middle East
13	Central Asia	13-01	2864	Hissar Alay
		13-02	12528	Pamir (Safed Khirs/W Tarim)
		13-03	10056	W Tien Shan
		13-04	3959	E Tien Shan (Dzhungaria)
		13-05	9435	W Kun Lun
		13-06	3667	E Kun Lun (Altyn Tagh)
		13-07	2252	Qilian Shan
		13-08	10821	Inner Tibet
		13-09	7008	S and E Tibet
14	South Asia (West)	14-01	2956	Hindu Kush
		14-02	21771	Karakoram
		14-03	9132	W Himalaya
15	South Asia (East)	15-01	7770	C Himalaya
		15-02	6908	E Himalaya
		15-03	7136	Hengduan Shan
16	Low Latitudes	16-01	2337	Low-latitude Andes
		16-02	2	Mexico
		16-03	4	E Africa
		16-04	2	New Guinea
17	Southern Andes	17-01	25357	Patagonia
		17-02	3976	C Andes
18	New Zealand	18-00	1162	New Zealand
19	Antarctic and Subantarctic[b]	19-01	151	Subantarctic (Pacific)

		19-02	3751	South Shetlands and South Orkneys
		19-03	2523	Subantarctic (Atlantic)
		19-04	954	Subantarctic (Indian)
		19-05	662	Balleny Islands
		19-11	2714	E Queen Maud Land 7A
		19-12	554	Amery Ice Shelf 7B
		19-13	2765	Wilkes Land 7C
		19-14	590	Victoria Land 7D
		19-15	2590	Ross Ice Shelf 7E
		19-16	0	Marie Byrd Land 7F
		19-17	17319	Pine Island Bay 7G
		19-18	14861	Bellingshausen Sea 7H1
		19-19	61169	Alexander Island 7H2
		19-20	9278	W Antarctic Pena 7I1
		19-21	6385	NE Antarctic Pena 7I2
		19-22	770	SE Antarctic Pena 7I3
		19-23	0	Ronne-Filchner Ice Shelf 7J
		19-24	5821	W Queen Maud Land 7K
		19-31	—	Antarctic Ice Sheet

a: Glaciers in region 10-03 (E Chukotka) are not in the RGI; the area is from Sedov, R.V. (1997), Ledniki Chukotki, *Materialy Glyatsiologicheskikh Issledovanij*, **82**, 213-217.

b: In region 19 (Antarctic and Subantarctic) some second-order regions are named after their sector of the mainland; there are no mainland outlines in the RGI.

Technical Specifications

Data are provided as shapefiles containing the outlines of glaciers in geographic coordinates (longitude/latitude, in degrees) and are referenced to the WGS84 datum. Data are organized by first-order region, with one shapefile containing all glaciers for each region. For some of the regions included in this dataset, more detailed information about the glaciers is available from the GLIMS database or in the World Glacier Inventory (WGI).

Glacier Delineation

Many glacier outlines were originally submitted as glacier complexes, that is, as collections of contiguous glaciers that meet at glacier divides. We used semi-automated algorithms (Bolch et al., 2010a; Kienholz et al., 2013) to delineate glaciers from these complexes. The quality of raw output from these algorithms primarily depends on the quality of the digital elevation model (DEM) available for a particular region. Even when a high-quality DEM is available the algorithm output requires some manual checking. These checks were not carried out for all RGI regions, and in many cases further work is necessary to inspect the quality of drainage divides.

Data Fields

Each glacier has 12 data attributes (10 in versions 1.0 and 2.0). The purpose of these fields is not to emulate the extensive sets of attributes found in the Global Land Ice Measurements from Space (GLIMS, Raup and Singh Khalsa 2007) database or the WGI, but only to offer convenient locational and identifying information.

RGIId

A 14-character identifier of the form RGI*vv-rr.nnnnn*, where *vv* is the version number, *rr* is the first-order region number and *nnnnn* is an arbitrary identifying code that is unique within the region. These codes were assigned as sequential positive integers at the first-order (not second-order) level, but they should not be assumed to be numbers In general the identifying code of each glacier, *nnnnn*, should not be expected to be the same in different RGI versions.

GLIMSId

A 14-character identifier in the GLIMS format G*xxxxxx*E*yyyyy*Ɵ, where *xxxxxx* is longitude east of the Greenwich meridian in millidegrees, *yyyyy* is north or south latitude in millidegrees, and Ɵ is N or S depending on the hemisphere. These identifiers were assigned by computing the centroid of the glacier polygon, and so are not guaranteed to lie within the glacier boundary. They do, however, agree with *CenLon* and *CenLat* (see below).

RGIFlag

This field was added in RGI version 3.0. It contains the text "Glacier" for glaciers, "Ice cap" for ice caps (in the Antarctic and Subantarctic only) or "Nominal" for glaciers whose outlines are nominal circles. For glaciers in the Greenland periphery it contains the text "CL*x*", where *x* is 0, 1 or 2 depending on the connectivity level of the glacier (explained under Region 5: Greenland Periphery below). In the Low Latitudes there remain a small number of unsubdivided glacier complexes for which *RGIFlag* contains "Complex".

BgnDate, EndDate

The date of the survey or image from which the outline was taken, in the form *yyyymmdd*, with missing dates represented by -9999999. When a single date is given in the source it is assigned to *BgnDate*. If only a year is given, *mmdd* is set to 9999. Only when the source provides a range of dates is *EndDate* not missing, and in this case the two codes together give the date range.

The form for missing dates was -9990000 in RGI versions 3.0 and earlier.

Slightly more than one half of the glacier complexes have date information (Figure 2).
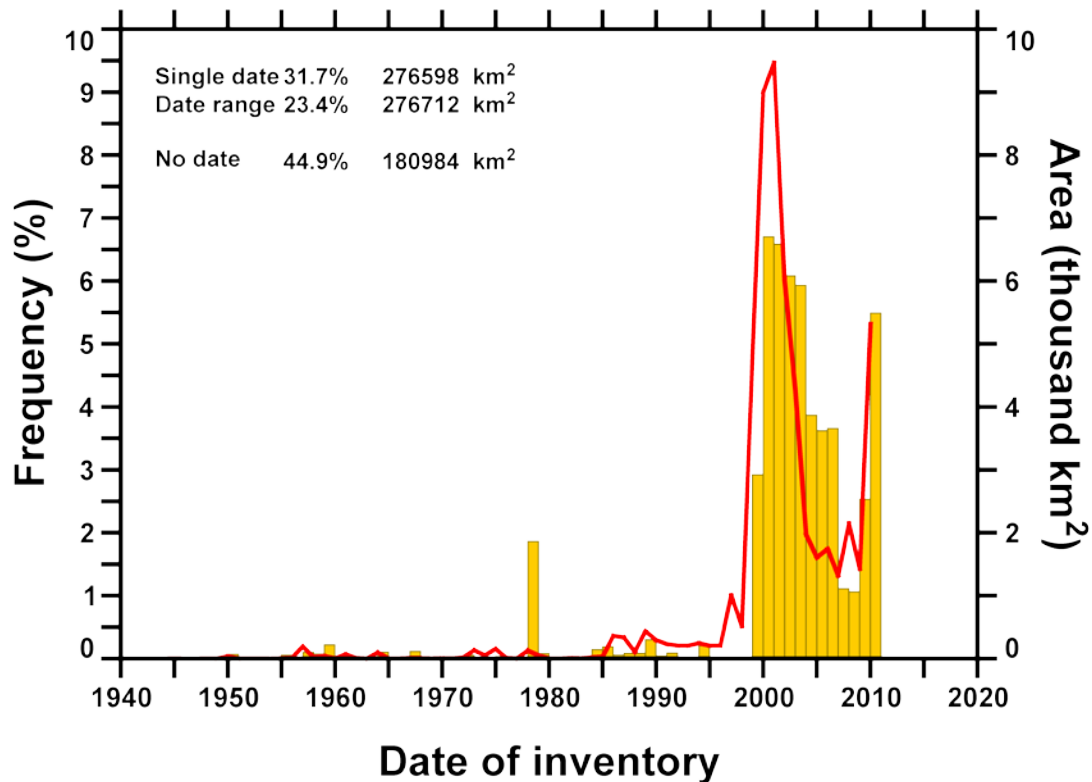

Figure 2. Frequency distribution of dates in the Randolph Glacier Inventory. Glaciers with date ranges are assigned with uniform probability to each year of the range. Undated glaciers in China date from the 1970s and 1980s and in Antarctica from the 1960s to 2000s. Most other undated glaciers are known to have been obtained from Landsat ETM+, ASTER or SPOT5 imagery, that is, of the 1990s or later.

CenLon, CenLat
Longitude and latitude, in degrees, of a point representing the geometric center of the glacier polygon. These coordinates agree with those in *GLIMSId*.

O1Region, O2Region
The codes of the first-order and second-order regions (Table 1) to which the glacier belongs.

Area
Area of the glacier in km^2.

GlacType
The GlacType field, added in RGI version 3.0, contains a four-digit glacier type code (ASCII text format) following the convention outlined in Table 1 of Paul *et al.* (2009).

Table 1. Codes for the four digits of the new remarks column in the GLIMS glacier database. Abbreviations: perim.: perimeter; spec. rem.: see specific remarks; not spec.: not specified.

Code	1: Snow	2: Calving	3: Surging	4: Divides
0	normal	normal	normal	normal
1	hides 5–50% of perim.	tidewater	reported	uncertain
2	hides >50% of perim.	freshwater	signs	compound
3	perennial snowfield	dry	signs & reported	ice cap
4	seasonal snowfield	regenerated	–	–
8	spec. rem.	spec. rem.	spec. rem.	spec. rem.
9	not spec.	not spec.	not spec.	not spec.

As of version 3.2, only the second digit, containing information on the Calving type, has been populated, with the exception of some glaciers in Alaska for which the third digit has also been populated to identify some surge-type glaciers. In the Antarctic and Subantarctic the code "5" has been added for digit 2 to represent shelf-terminating glaciers.

Name
Name of the glacier, or the WGI or WGI-XF id code if available. Nearly all glaciers lack this information.

Quality Control
A series of quality checks are conducted on all glacier polygons before they are released. These include geometry, topology and attribute field checks. As of version 3.2, the following steps are carried out:

1) The ArcGIS "repair geometry" tool is run on all polygons. Among other tasks, this routine checks for polygon closure, corrects the ring ordering and eliminates duplicate verticies. The full list of geometry checks is given here: (http://resources.arcgis.com/en/help/main/10.1/index.html#/Repair_Geometry/00170000003v000000/)
2) Glaciers with areas less than 0.01 km^2 are removed. Nunataks are retained whatever their area.
3) A common error occurs when glacier polygons are adjusted during an editing process without ensuring that the shared boundary with an adjacent polygon is also updated (for example, at a glacier divide). Such errors result in overlapping polygons, or gaps between polgyons, yielding small "sliver" polygons that must be removed or corrected. To check for these errors we constructed topology rules within ESRI's ArcGIS 10.1. We began by checking topology using the "does not overlap" rule. Next, we removed each glacier with errors and wrote it to its own single polygon shapefile. In an iterative procedure, each single glacier was updated on all others, such that areas with overlap were eliminated. The final subset of glaciers was merged back into the error-free outlines, creating a new set of outlines without topology errors.
4) Attribute tables are checked using a series of scripts written in Python. The scripts look for things like empty fields or incorrectly formatted dates.

DESCRIPTION OF DATA COMPILATION BY REGION

REGION 1: Alaska

Contributor	Institution	Project/Funding
Arendt, A.	University of Alaska, Fairbanks, USA	National Park Service, Geophysical Institute, NASA Cryospheric Sciences, Geographic Information Network of Alaska
Herreid, S.		
Hock, R.		
Kienholz, C.		
Rich, J.		
Beedle, M.	University of Northern British Columbia, Canada	
Berthier, E.	CNRS-OMP-LEGOS, France	
LeBris, R.	University of Zurich, Switzerland	GlobGlacier funded by ESA
Frey, H.		
Paul, F.		
Bolch, T.		
Burgess, E.	University of Utah, USA	
Forester, R.		
Lund, J.		
Giffen, B.	National Park Service, USA	
Hall, D.	NASA Goddard Space Flight Center, USA	
Manley, W.	INSTAAR, USA	

The Alaska region encompasses all glaciers in the state of Alaska, USA, as well as all glaciers in the Yukon Territory and British Columbia, Canada, that are part of the icefields that straddle the US/Canada Border. On its southeastern boundary, the region ends just north of Prince Rupert, British Columbia and just south of the end of the Alaska border. From there the region extends inland to the divide between Gulf of Alaska and Arctic drainages.

Version 1.0:
Numerous groups have contributed Alaska glacier outlines. Le Bris et al. (2011) mapped the Kenai Peninsula, Tordillo, Chigmit and Chugach Mountains using Landast TM scenes acquired between 2005-2009. They used automated (band-ratioing) glacier mapping techniques with additional manual editing to deal with incorrect classification of debris-covered glaciers. Drainage divides in the accumulation region were derived from the USGS DEM.

As part of a mapping effort by the National Park Service (NPS), the University of Alaska Fairbanks (UAF) has been mapping all glaciers in NPS boundaries, as well as glaciers connected to but not within park boundaries, for two time periods (USGS 1950s map dates, and most recent satellite imagery). For this effort UAF has in many regions started with existing, older outlines and updated them to the most modern imagery available. These include outlines from Berthier (Berthier et al., 2010), Beedle (Beedle et al., 2007), Giffen, Hall and Manley. UAF has updated these outlines to circa 2010 pan-sharpened 15 m resolution Landsat 7 ETM+ scenes, 5 m resolution imagery from the SPOT SPIRIT initiative (dating approximately 2007; Korona et al., 2009) and 2006-2010 IKONOS imagery. UAF Geophysical Institute internal funding has also been used to support digitizing efforts in the Alaska Range, Chugach Mountains and Juneau Icefield glaciers. Nearly all of these regions are based on 2010 imagery.

The University of Utah (Burgess, Forester, Lund) created outlines for the Stikine Icefield region derived from 1980s Landsat 5 imagery.

Manley provided all outlines for Brooks Range glaciers.

Glaciers along the Aleutian Island chain are taken from Berthier et al. (2010).
Glaciers other than those mapped by Le Bris et al. (2011) were delineated using an automated algorithm developed by C. Kienholz (Kienholz et al., 2013). USGS digital elevation models as well as the ASTER GDEM v1 were used as sources of elevation information for the algorithm.

Changes from Version 1.0 to Version 2.0:

Glaciers in Katmai and Lake Clark National Parks have been updated to 2006-2010 IKONOS imagery.

Portions of the Stikine Icefield region have been improved by removing misidentified small glaciers around the periphery of the icefield.

Glaciers at the head of Lynn Canal, and in the eastern portion of the Western Chugach Mountains near Cordova, have been updated.

Extensive improvements have been made to the Wrangell/St. Elias region. What is included in RGI version 2.0 is a partially edited version of Berthier et al.'s (2010) and Beedle et al.'s (2007) outlines, updated to circa 2010 Landsat 7 ETM+ imagery for the Wrangell Mountains, 2006-2010 IKONOS imagery for the US portion of St. Elias, and Canadian topographic maps for the Canadian portion of the St Elias. Between V1.0 and V2.0 we have focused on capturing the largest area changes occurring primarily at low elevations, however some regions remain unmodified between V1.0 and V2.0 (Figure 3).

Changes from Version 2.0 to 3.0
Additional improvements were made to the St.Elias, Lake Clark and Juneau Icefields regions. All remaining DCW outlines were replaced with modern outlines.

Changes from Version 3.0 to 3.2:

Manual checks were carried out to improve the quality of glacier divides. Some divides were re-digitized in this process. This changed the total number of glaciers in the Alaska region.

Glaciers of the Western Chugach Mountains were edited, primarily to fix regions misclassified as glacier at high elevations. This editing resulted in a small change in total area for the Western Chugach Mountains region.
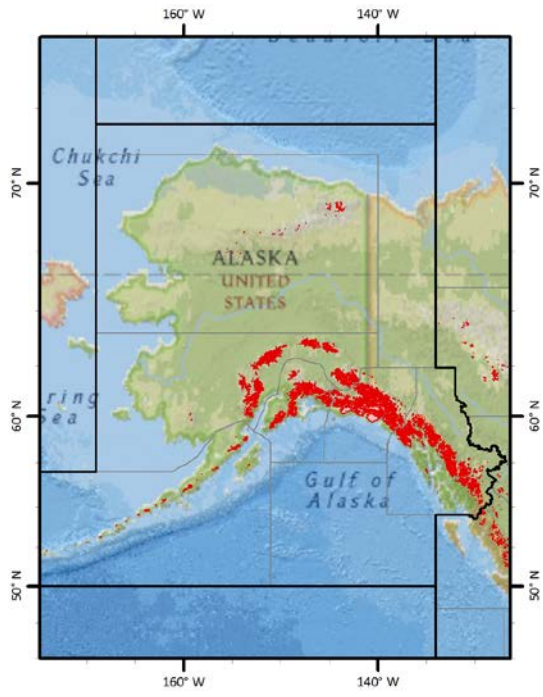
REGION 2: Western Canada and US

Contributor	Institution	Project/Funding
Bolch, T.*	UNBC, Canada * now at: University of Zurich, Switzerland	WC2N funded by CFCAS
Menounos, B.		
Wheate, R.		
Fountain, A.	Portland State University, USA	

Version 1.0

Glaciers in BC and Alberta were mapped using orthorectified Landsat 5 TM scenes from the years 2004 and 2006 obtained by British Columbia Government, Ministry of Forests and Range. We selected the TM3/TM5 band ratio for glacier mapping. For the entire study area, we used improved British Columbia TRIM glacier outlines as a mask to minimize misclassification due to factors such as seasonal snow. When using this mask, we assumed that glaciers did not advance between 1985 and 2005, an assumption that holds for practically all non-tidewater glaciers in western North America. The mask also maintained consistency in the location of the upper glacier boundary and the margins of nunataks. This consistency is important in case of seasonal snow that hampers correct identification of the upper glacier boundary. We mapped only glaciers larger than 0.05 km^2 as a smaller threshold would include many features that were most likely snow patches. In addition, all snow and ice patches that were not considered to be perennial ice in the TRIM data were eliminated and hence, we minimize deviations in glacier areas that could arise from interpretative errors or major variations in snow cover. The resulting glacier polygons were visually checked for gross errors based on the procedures previously discussed, and overall, fewer than 5% of the glaciers were manually improved. We derived glacier drainage basins based on a flowshed algorithm using the TRIM DEM and a buffer around each glacier. More information can be found in Bolch et al. (2010a).

Data for the remaining US locations were derived from the GLIMS database. Metadata are located at http://glaciers.us.

Changes from Version 1.0 to Version 2.0:
The glaciers on Melville Island (region 02.01) were represented in version 1.0 by DCW outlines and have been replaced by Canvec outlines taken from Region 03. DCW outlines for the Mackenzie Mountains and Selwyn Mountains (region 02-02), on the boundary between Yukon and the North West Territories, were replaced by Canvec outlines provided by M. Sharp and J.G. Cogley.

Changes from Version 2.0 to Version 3.0
Glaciers were delineated from glacier complexes in the northern part of this region.

No changes were made from Version 3.0 to 3.2

REGIONS 3 and 4: Arctic Canada North and Arctic Canada South

Contributor	Institution	Project/Funding
Gardner, A.	Clark University, USA	
Wolken, G.	Department of Geological and Geophysical Surveys, Alaska, USA	
Barrand, N.		
Cawkwell, F.		
Copland, L.		
Filbert, K.		
Hartmann, G.	University of Alberta, Canada	
O'Callaghan, P.		
Sharp, M.		
Wyatt, F.		
Burgess, D.	Natural Resources Canada	
Paul, F.	University of Zurich, Switzerland	GlobGlacier funded by ESA

Region 3: Arctic Canada North

Glacier outlines were created from late summer, cloud free 1999-2003 Landsat 7 (ETM+) imagery and from 2000-2003 ASTER imagery. A normalized-difference snow index (NDSI) was calculated for all Landsat imagery to classify all snow and ice covered terrain. Empirically derived thresholds were applied to refine these classifications and isolate snow and glacier ice components. A clumping procedure was then applied to the classified snow and ice data to delineate contiguous groups of pixels, followed by an elimination procedure, which removed small clusters of non-ice pixels. Gridded snow and ice data were then converted to polygons and edited manually to correct misclassifications. Small portions of some areas within this region were not adequately imaged by Landsat, due to either persistent cloudiness or shadowing. Consequently, in these areas manual (heads-up) digitization of ASTER imagery was used to capture glacier outlines.

Outlines for Devon Island were provided by D. Burgess and were derived from 1999/2000 velocity maps.

Changes from Version 1.0 to Version 2.0:

Canvec outlines of the Melville Island glaciers, which were mistakenly duplicated in region 03 in version 1.0, were transferred to region 02.

Changes from Version 2.0 to 3.2:

Only a portion of glaciers were delineated in version 2.0. At version 3.2, all glaciers were delineated from glacier complexes.

**Region 4: Arctic Canada South**

Glacier complex outlines were compiled from 214 CanVec maps, a digital cartographic reference product produced by Natural Resources Canada. An additional 5500 km^2 of glacier area in central Baffin Island not covered by Edition 9 of the CanVec data set were taken from an expanded inventory based on Paul and Kääb (2005) and Svoboda and Paul (2009). All outlines in this expanded

inventory were created from late-summer Landsat 7 ETM+ imagery acquired between 1999 and 2002. Of the CanVec maps, 13 were based on late-summer SPOT 5 imagery acquired between 2006-2010 and seven on 1958 or 1982 aerial photographs. A small fraction of ice coverage is missed by the Canvec dataset because of incorrect classification over debris covered ice and supraglacial lakes. The misclassification is very noticeable for outlet glaciers where medial moraines are not identified as glacier ice. Glaciers were delineated using a basin delineation algorithm developed by C. Kienholz (Kienholz et al., 2013). Note that these are raw outputs from the delineation algorithm and need to be edited. Users are encouraged to contact RGI data coordinators if they wish to assist in merging and cleaning polygons to improve this dataset.

Changes from Version 1.0 to Version 2.0:
Outlines for 27 glaciers in Labrador (region 04-09) were added, provided by P. O'Callaghan, N. Barrand, F. Wyatt, M. Sharp, University of Alberta.

No changes were made from Version 2.0 to 3.2
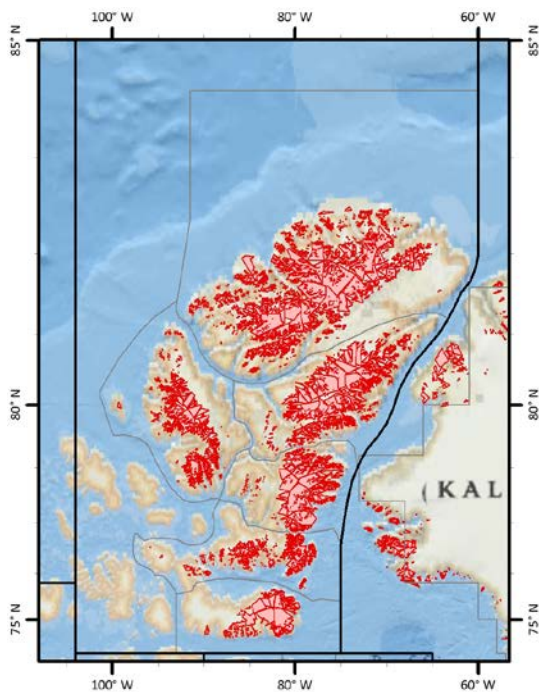
REGION 5: Greenland Periphery

Contributor	Institution	Project/Funding
Bolch, T.	University of Zurich, Switzerland	ice2sea funded by EU FP7 GlobGlacier funded by ESA Glaciers_cci funded by ESA
Rastner, P.		
Moelg, N.		
LeBris, R.		
Paul, F.		
Howat, I.	Byrd Polar Research Center, Ohio State University, USA	
Negrete, A.		

There are numerous glaciers in the periphery of the Greenland ice sheet. Distinguishing between what is considered ice sheet versus glaciers is a challenge, and depends on the scientific application. While the distinction is clear for the numerous fully detached glaciers, there are several regions where, although there is a physical connection to the main ice sheet, the ice mass is either a valley glacier in mountainous terrain, or it forms its own ice dome and is largely uncoupled to the ice sheet dynamics. Therefore, for applications such as extrapolation of laser altimetry data, some researchers believe such ice masses should be categorized as glaciers rather than as part of the ice sheet.

In the RGI, all ice masses with a possible but uncertain drainage divide are assigned to the ice sheet (e.g. on the Geikie Plateau), and all others to the local (or peripheral) glaciers. The latter are either:

- not connected to the ice sheet at all
- clearly separable (e.g. by mountain ridges) in the accumulation region, or
- only in contact with ice sheet outlets in the ablation region.

Indeed, there is room for discussion on individual decisions, but for the purpose of the RGI we just need to start somewhere. The separation in the accumulation area is done along drainage divides derived from DEM-based watershed analysis.

The glaciers north of ~81°N were not available from Landsat data and were provided by the Greenland Mapping Project (Howat and Negrete, in prep).

The semi-automated glacier mapping applied to the 64 Landsat scenes that were processed is based on a band ratio (ETM+ band 3 / 5) with an additional threshold in band 1 for better mapping of glacier areas in cast shadow. It is based on Paul and Kääb (2005) and described for a part of western Greenland in Citterio et al. (2009). Debris-covered glacier parts as well as wrongly classified sea ice, icebergs or lakes were corrected manually in the vector domain. A 3 by 3 median filter is applied for image smoothing and glaciers smaller than 0.05 km^2 are not considered. Wrongly classified regions with seasonal snow could not always be corrected.

Changes from Version 1.0 to Version 2.0:
No changes were made.

Changes from Version 2.0 to Version 3.0:
Coverage of Greenland is new in version 3.0, and is described in detail by Rastner et al. (2012). In all, 73 satellite images were processed. Glacier complexes were subdivided using a flowshed algorithm. An enhanced form of the algorithm for identifying glaciers other than the Greenland Ice Sheet was developed. In addition to the connectivity rule described above, a "topographic heritage rule" was added. Glaciers adjoining the ice sheet were first assigned to level CL2 (strongly connected) or level

CL1 (weakly connected). Unassigned glaciers adjoining one or more level-2 glaciers were then assigned the same connectivity, and likewise for glaciers adjoining level-1 glaciers. The remaining unassigned glaciers, those not connected to the ice sheet at all, were assigned to level CL0. The result of these operations is summarized in Table2.

Table2. Number and extent of glaciers in Greenland

Connectivity Level	Number	Area (km^2)
CL0	16 655	65 146 ± 2019
CL1	1 771	24 127 ± 2747
CL2	1 855	40 710 ± 1262
Ice sheet	1	1 678 497 ± ????
Total	20 282	1 808 480 ± 4028

Glaciers of all three connectivity levels are included in RGI version 3.0. Rastner et al. recommend that CL2 glaciers be treated as part of the ice sheet, for which purpose they can be identified using the new data field *RGIFlag*. The total extent of CL0 and CL1 glaciers, 89273 km^2, is well in excess of any previous estimate of the extent of glaciers in the Greenland periphery. Adding the CL2 glaciers and the ice sheet, Rastner et al. estimate a glacierized area for Greenland as a whole of 1.808±0.004 × 10^6 km^2. This lies between the two estimates suggested by Kargel et al. (2012), 1.801±0.016 × 10^6 km^2 and 1.824±0.016 × 10^6 km^2; these estimates are statistically indistinguishable from but more uncertain than that of Rastner et al.

Changes from Version 3.0 to 3.2
A planimetric offset was discovered in parts of Greenland in version3.0. This offset was repaired.
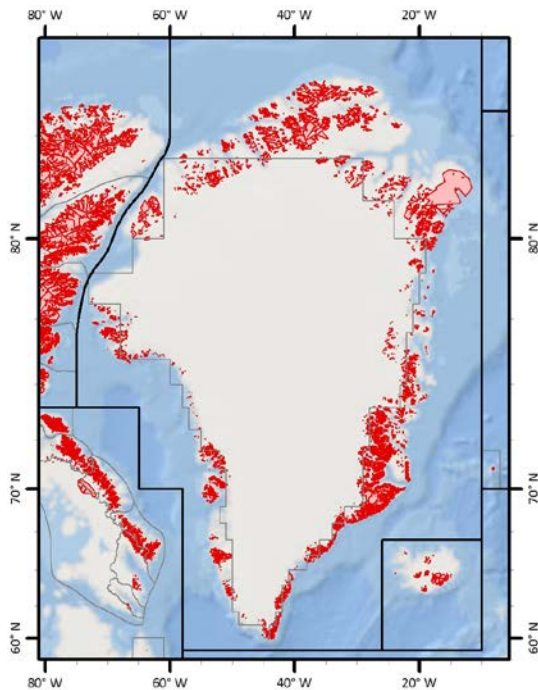
REGION 6: Iceland

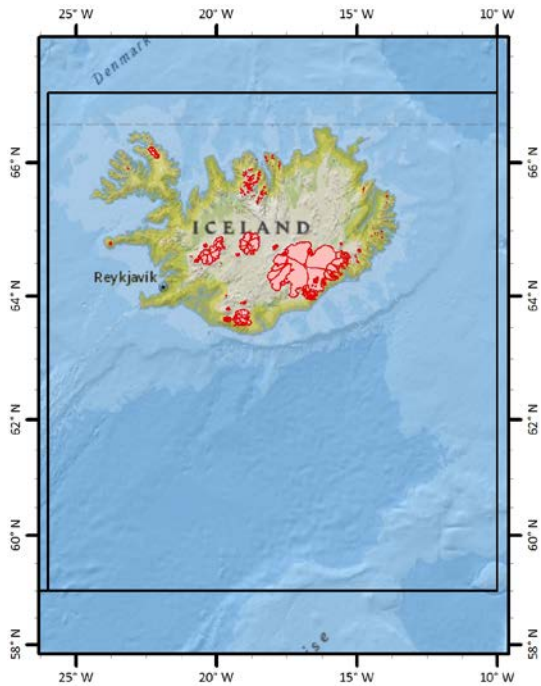| Contributor	Institution	Project/Funding
Sigurðsson, O.	National Energy Authority, Iceland	

Outlines of glacier complexes in Iceland were added to the GLIMS database by O. Sigurðsson and extracted therefrom by G. Cogley, who merged nunataks with the glacier complexes containing them. Most outlines were acquired from 1999-2004 ASTER and SPOT5 imagery; some in the north of Iceland were acquired from oblique aeriaal photographs.

Changes from Version 1.0 to Version 2.0:

No changes were made.

Changes from Version 2.0 to Version 3.2:

Glaciers were delineated from the glacier complexes.

REGION 7: Svalbard

Contributor	Institution	Project/Funding
Koenig, M. Kohler, J.	Norwegian Polar Institute, Norway	Cryoclim funded by ESA
Hagen, J-O.		Cryoclim and Glaciers_cci funded by ESA
Nuth, C.		
Moholdt, G.	University of Oslo, Norway	
Pettersson, R.	Uppsala University, Sweden	

Three primary data sets are used to compile the glacier inventory of Svalbard. The main sources are SPOT5-HRS DEMs and orthophotos provided within the framework of the IPY-SPIRIT (SPOT 5 stereoscopic survey of Polar Ice: Reference Images and Topographies) Project (Korona et al., 2009). The SPOT5-HRS collects 5m panchromatic stereo images that are stereoscopically processed into 40m DEMs, then used for the orthophoto generation of the original images. Five SPIRIT scene acquisitions from 2007-2008 cover 71% of the glacier area. The secondary sources are from the ASTER sensor in the form of automatically generated DEMs and orthophotos (AST14DMO products downloaded from NASA). These have a narrower swath (60 km), and therefore 23 scenes are used to cover 16% of the glacier area. Cloud-free scenes are not available for 2007-2008, and therefore data from as early as 2001 are used. For less than 14% of the glacier area, a suitable SPOT5-HRS or ASTER scene was not available. For these glaciers, 11 orthorectified Landsat scenes are used. Furthermore, additional Landsat and ASTER scenes are used to aid digitization decisions about the seasonal snow cover.

The original glacier delineation and glacier identification system is based on the Hagen et al. (1993) atlas, which conforms to WGI standards but is only available as a hard-copy rather than GIS data. Therefore, digitized national datasets are the base glacier masks from which to begin the inventory (König et. al, 2013). From this original dataset, we manually re-delineated the individual glacier basins based upon the Hagen et al. (1993) *Atlas* and updated by trimming the front position and the lateral edges below the ELA. Since the original national dataset was derived by cartographers, many of the mask segments above the ELA contained snow covered valley walls and gullies (not perennially snow covered). These are, to the best of our ability, clipped from the masks by visually analyzing the recent satellite archives of ASTER and Landsat.

The Svalbard inventory is described in more detail by Nuth et al. (2013).

Figure 4 summarizes the distribution of imagery dates used to generate the Svalbard outlines.

Changes from Version 1.0 to Version 2.0:
Outlines of the glaciers on Jan Mayen (07-02) were digitized by J.G. Cogley from Hagen et al. (1993).

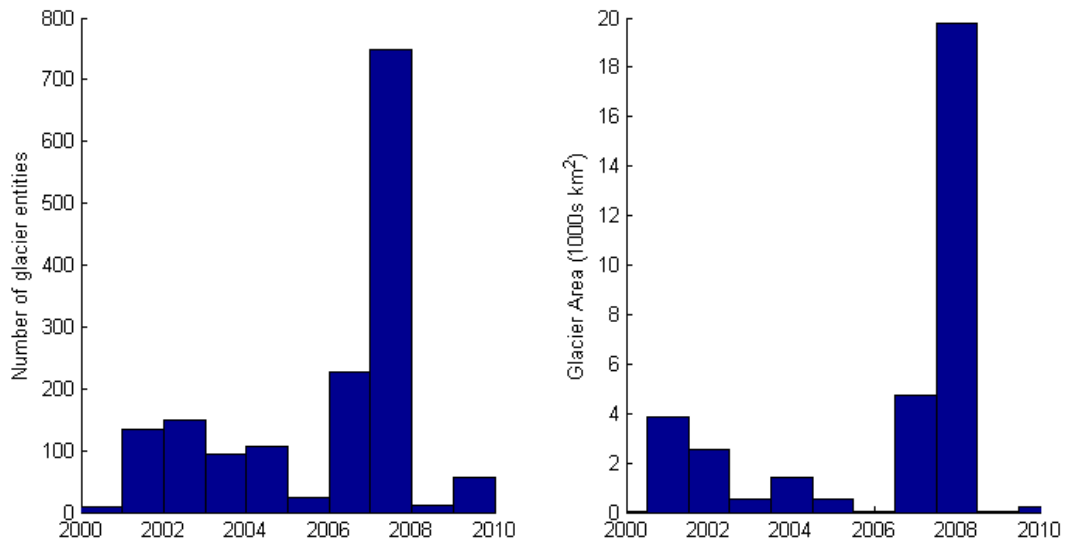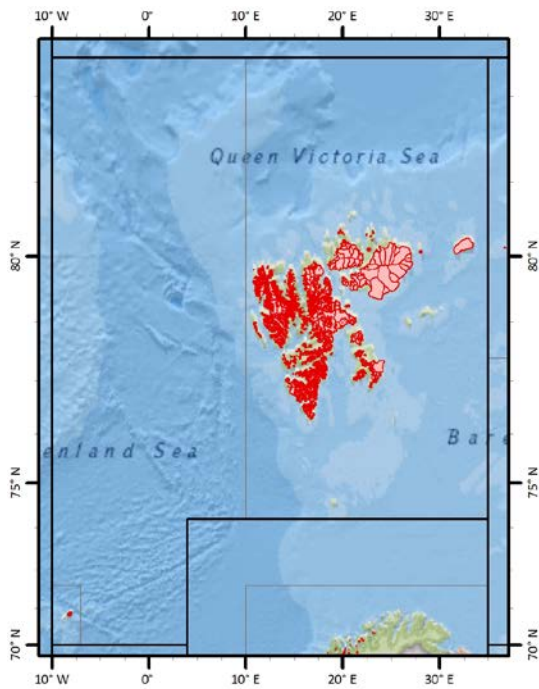**No changes were made from Version 2.0 to 3.2**

Figure 4. Time distribution of the imagery used to generate the Svalbard portion (Region 7) of the RGI, showing the number of glaciers (left) and the total glacier area (right) as a function of image year.

REGION 8: Scandinavia

Contributor	Institution	Project/Funding
Andreassen, L.	Norwegian Water Resources and Energy Directorate, Norway	
Winsvold, S.		
Hagen, J-O.	University of Oslo, Norway	
Paul, F.	University of Zurich, Switzerland	GlobGlacier funded by ESA
Mercer, A.		
Brown, I.	University of Stockholm, Sweden	

The glacier outlines for Norway are based on Landsat (TM and ETM+) imagery from 1999-2006.

The Swedish glacier outlines use imagery from SPOT5 and SPOT4 (dates not provided). In some regions these outlines were updated against September 2008 Swedish Land Survey imagery available on Google Earth.

The glacier mapping to which GlobGlacier contributed is documented in Andreassen et al. (2008) for Jotunheimen, Paul and Andreassen (2009) for Svartisen, and Paul et al. (2011) for the Jostedalsbreen region.

Changes from Version 1.0 to Version 2.0:
Four glaciers in the Khibiny Mountains of the Kola Peninsula (08-02) were added as nominal circles from WGI-XF.

Changes from Version 2.0 to 3.2:
Glaciers were delineated from glacier complexes.
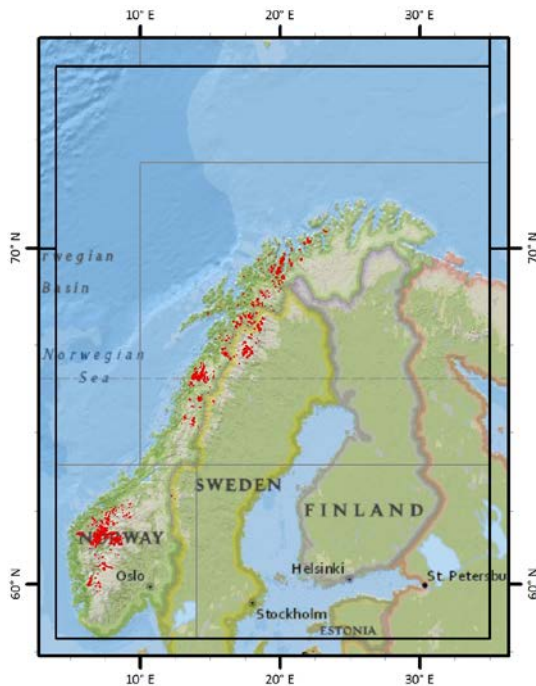
REGION 9: Russian Arctic

Contributor	Institution	Project/Funding
Moholdt, G.	University of Oslo, Norway	ice2sea, grant number 226375

This basic inventory was constructed as a part of a mass balance study of the Barents/Kara Sea region in the Russian High Arctic (Moholdt et al., submitted). It covers all glaciers and ice caps in Novaya Zemlya (22,100 km^2), Severnaya Zemlya (16,400 km^2), Franz Josef Land (12,700 km^2), Ushakov Island (320 km^2) and Victoria Island (6 km^2). Glacier complexes were manually digitized from orthorectified satellite imagery acquired during summers between 2000 and 2010. SPIRIT SPOT5 scenes (Korona et al., 2009) were used for most of Novaya Zemlya, while the best available Landsat scenes were used elsewhere. All visible nunataks were cut out from the glacier polygons, and snowfields were only included if they seemed to be a part of a glacier. Ice shelves in Franz Josef Land (<50 km^2) were included as parts of the glacier polygons, while the Matusevich Ice Shelf in Severnaya Zemlya (~200 km^2) was delineated into a separate polygon. The estimated total glacier area of the region (51,500 km^2) is 9% smaller than that of the World Glacier Inventory (Ohmura, 2009). This large deviation is probably due to a combination of long-term glacier retreat and methodological differences in glacier delineation.

Changes from Version 1.0 to Version 2.0:
The Matusevich Ice Shelf, which would have been the only ice shelf in the inventory, was removed.

No changes were made from Version 2.0 to 3.2
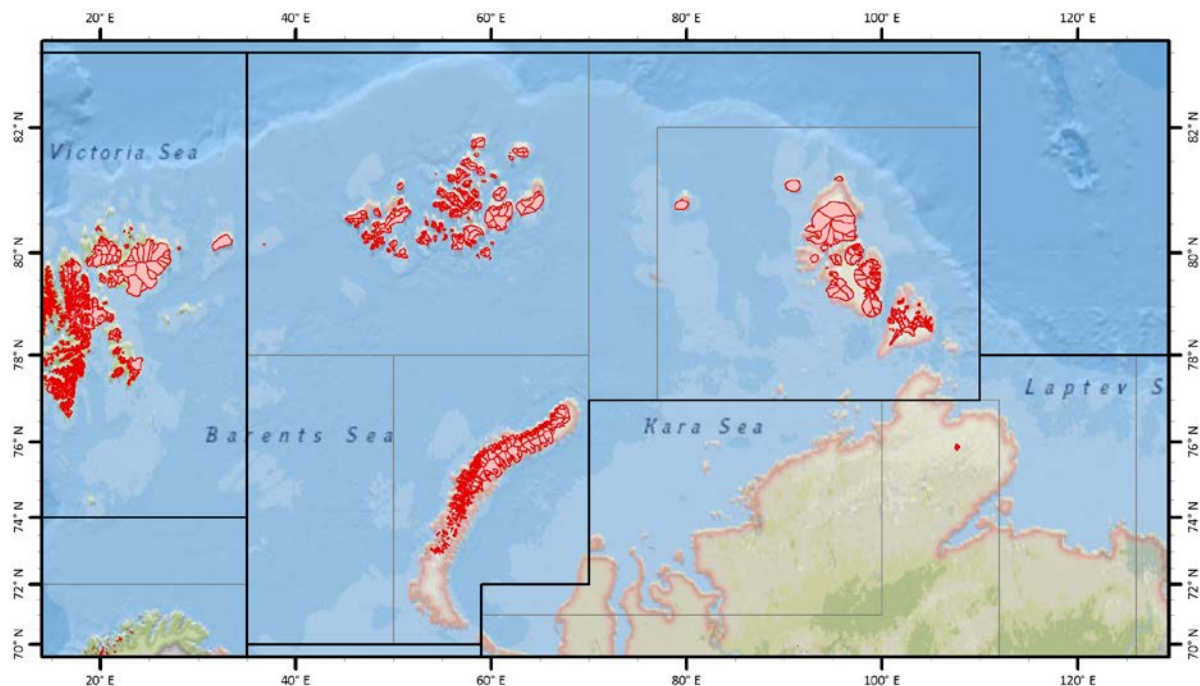
REGION 10: North Asia

Contributor	Institution	Project/Funding
Stokes, C., Gurney, S.	Durham University, UK	
Khromova, T.	Institute of Geography, Russian Academy of Science, Moscow, Russia	

About one third of the glacier outlines in North Asia were manually delineated from Landsat TM/ETM+ or ASTER imagery. Missing areas were filled by a glacier layer compiled by B. Raup (Raup et al., 2000) from the Digital Chart of the World (DCW) and the World Glacier Inventory (WGMS, 1989; Haeberli et al., 1998).

The WGI data base locates each glacier with only a geographical point rather than a polygon. These glaciers are presented as circular polygons of the area given in the WGI.

Changes from Version 1.0 to Version 2.0:

The DCW outlines of glacier complexes in Mongolia were replaced by outlines of glaciers digitized by J.G. Cogley from Soviet military maps. Their dates range between 1968 and 1983.

14 glaciers in the Tajgonos Peninsula, northwest of Kamchatka (10-02) were added as nominal circles from WGI-XF.

The information available for Chukotka (10-02 and 10-03; Sedov 1997) did not include locations of individual glaciers, and so they do not appear in the RGI. Their total area is 17.1 km^2.

Changes from Version 2.0 to Version 3.0:

All of the glaciers represented as circles were regenerated from WGI-XF (Cogley 2009). Some of them have not just nominal shapes but nominal positions, being derived from the Soviet *Katalog Lednikov*, which in each drainage basin gives full information only for glaciers larger than 0.1 km^2. Only a total number and total area are given for glaciers smaller than 0.1 km^2. In WGI-XF these small glaciers are all assigned a common position roughly in the centre of their basins, and an equal share of the listed small-glacier area. Obviously these and other nominal glaciers should not be used for purposes other than calculating total glacierized area.

Some DCW outlines were found to overlie mountain ranges whose ice cover was already represented by nominal glaciers. These duplicate DCW outlines were removed.

**No changes were made from Version 2.0 to 3.2**

REGION 11: Central Europe

Contributor	Institution	Project/Funding
Frey, H.		
LeBris, R.	University of Zurich, Switzerland	GlobGlacier funded by ESA
Paul, F.		

The glacier outlines for this region are derived from ten Landsat TM images acquired during 2 months in the summer of 2003 using band ratio images. Drainage divides for individual glaciers were derived from the void-filled SRTM DEM (from CGIARS) in a resampled version with 60 m spatial resolution. All further details are documented in Paul et al. (2011b). About 30-50 km^2 of glaciers are not mapped, mainly very small glaciers located in Italy (Brenta and Dolomites) and Germany, covered by debris or located under local orographic clouds. A more complete version is planned for RGI 2.0. The original data sets (in UTM projection) can be downloaded from the globglacier.ch website (link Data access).

Changes from Version 1.0 to Version 2.0:

109 glaciers in the Pyrenees, and one in the Apennines, were added as nominal circles from WGI-XF. Together they constitute region 11-02.

No changes were made from Version 2.0 to 3.2
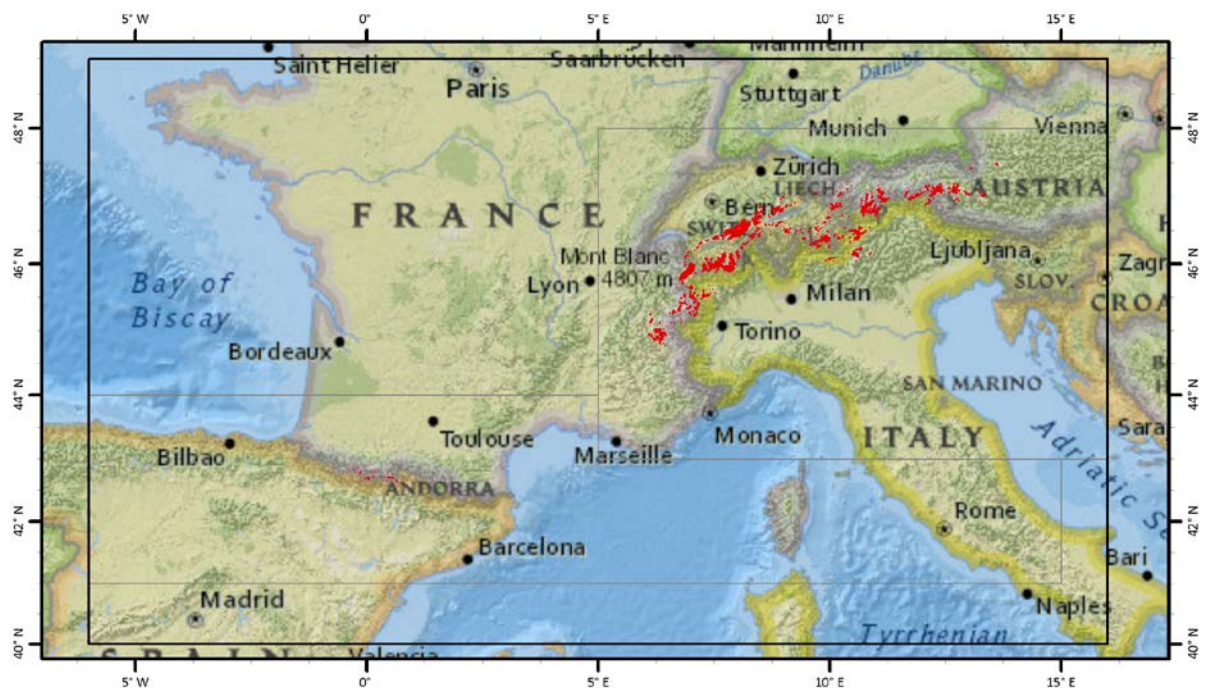
REGION 12: Caucasus and Middle East

Contributor	Institution	Project/Funding
Khromova, T.	Institute of Geography, Russian Academy of Science, Moscow, Russia	

The Caucasus is covered by the database of the Global Land Ice Measurements from Space initiative (GLIMS) (Raup et al., 2007).

Changes from Version 1.0 to Version 2.0:
The 37 glaciers of Iran (12-02) were added as nominal circles from Moussavi et al. (2009).

The information available for Turkey (Kurter 1991) was not adequate for placing the individual glaciers, which have a total area of 22.9 km^2.

Changes from Version 2.0 to 3.2:
Outlines of the glaciers of Turkey were provided by M.A. Sarıkaya (Sarıkaya and Tekeli, 2013).

REGION 13: Central Asia

Contributor	Institution	Project/Funding
Bolch, T.	Technische Universität Dresden, Germany; University of Zurich, Switzerland	DynRG-TiP and Aksu-Tarim-RS funded by the German Research Foundation (DFG)
Mölg, N.		
Kriegel, D.	GFZ Potsdam, Germany	CAWa, German Federal Foreign Office
Hagg, W.	LMU Munich, Germany	
Mayer, C.	Commission for Glaciology, Munich	
Khromova, T.	Institute of Geography, Russian Academy of Science, Moscow, Russia	

Large parts of Central Asia are covered by the database of the Global Land Ice Measurements from Space initiative (GLIMS). The GLIMS database consists in China of data from the first Chinese glacier inventory (Shi et al., 2009) and is of heterogeneous and generally slightly lower quality (more generalized) than the other glacier data used here. It has also to be noted that some of the GLIMS data in Central Asia have a shift in location. Large parts of the Tien Shan in Kazakhstan and Kyrgyzstan were mapped semi-automatically using ratio images from ASTER data (e.g. Kutuzov and Shahgedanova, 2009). Important missing areas such as the Central Pamirs, Naryn basin, northern Tien Shan (Bolch, 2007) and the Dzhungarian Alatau were mapped semi-automatically with manual corrections using Landsat TM/ETM+ scenes. The glacier inventory for the Nyainqentanglha Range in Tibet was taken from Bolch et al. (2010b).

Remaining missing areas were filled by a glacier layer compiled by B. Raup (Raup et al., 2000) from the Digital Chart of the World (DCW) and the World Glacier Inventory (WGMS, 1989; Haeberli et al., 1998). The DCW outlines are in western Kyrgyzstan (region 13-03), the Hissar Alay (13-01), the Safed Khirs (northern Afghanistan) and parts of the southwest Pamir (13-02).

The WGI data base locates each glacier with a geographical point rather than a polygon. These glaciers are presented as circular polygons of the area given in the WGI.

Changes from Version 1.0 to Version 2.0:
No changes were made.

No changes were made from Version 2.0 to 3.2
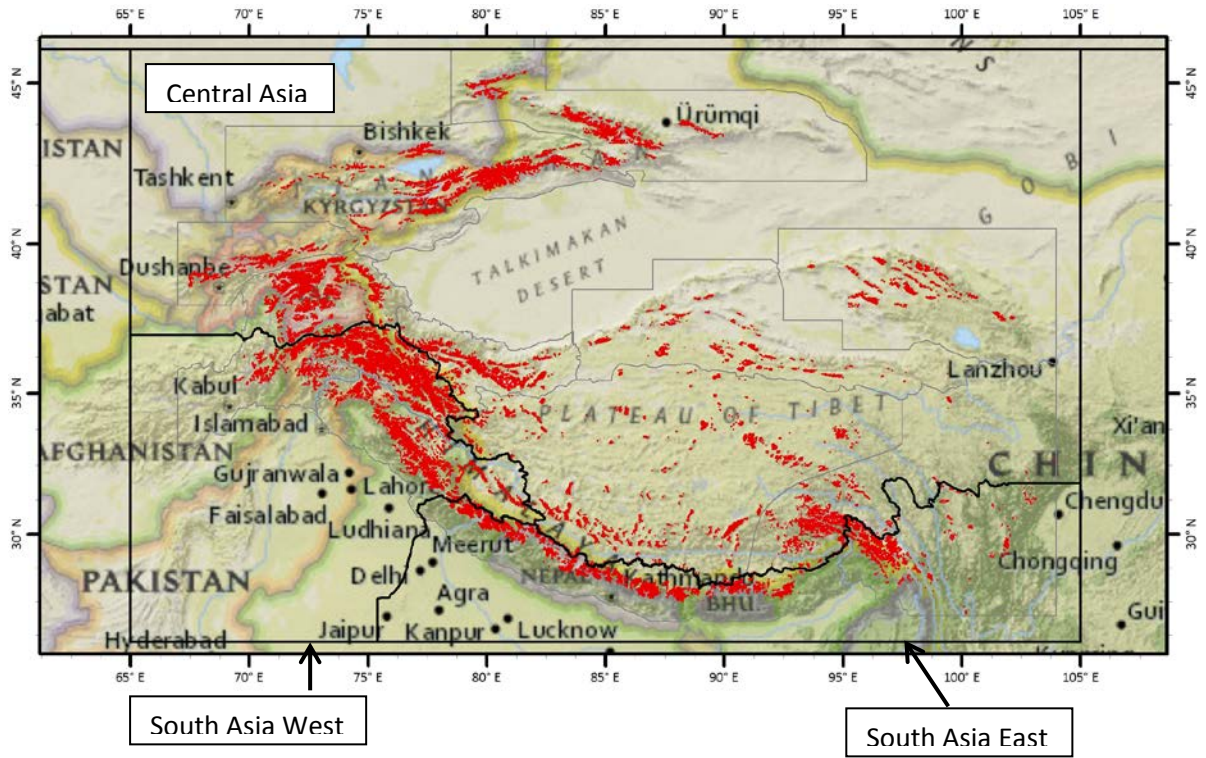
REGIONS 14 and 15: South Asia West and South Asia East

Contributor	Institution	Project/Funding
Bolch, T.		
Frey, H.	University of Zurich, Switzerland	GlobGlacier funded by ESA
Paul, F.		
Bajracharya, S.	ICIMOD, Nepal	
R. Bhambri	Center for Glaciology, Wadia Institute of Himalayan Geology, Dehradun India	

Large parts of the Himalaya, Karakoram and Pamir are covered by the database of the Global Land Ice Measurements from Space initiative (GLIMS) (Raup et al., 2007). For the present study, GLIMS data was used in cases where no other data was available, mainly on the northern slopes of the Himalayas and the northeastern part of the Karakoram. In these regions, the GLIMS database consists mostly of data from the first Chinese glacier inventory (Shi et al., 2009) and is of heterogeneous and generally slightly lower quality than the other glacier data used here. Glacier outlines compiled by the International Centre for Integrated Mountain Development (ICIMOD) were used for parts of the Karakoram, as well as the central and eastern Himalayas (ICIMOD, 2007, DVD). For Nepal, more recent data from 2008 and 2009 is available and was used here (ICIMOD, 2011, DVD). For parts of northwestern India, glacier inventory data compiled by the GlobGlacier project of the European Space Agency (ESA) (Paul et al., 2009) was used; the information was compiled from Landsat ETM+ and ALOS PALSAR data (Frey et al., in rev.). For a few regions in the Karakoram, no suitable glacier data was available. We therefore compiled new glacier outlines in these regions based on Landsat ETM+ data from the years 2002, 2009, and 2010.

No changes were made from Version 1.0 to Version 2.0

Changes from Version 2.0 to Version 3.2:
Outlines of the glaciers of Burma, provided by S. Bajracharya, were added to region 15.

REGION 16: Low Latitudes

Contributor	Institution	Project/Funding
Sharp, M.	University of Alberta, Canada	
Wyatt, F.		
Miles, E.	University of British Columbia, Canada	

In South America, shapefiles were created from late summer, cloud free Landsat 7 ETM+ imagery acquired prior to the 2003 scan line corrector (SLC) failure. To identify glacier surfaces, a normalized difference snow index (NDSI) was calculated using bands 5 and 2 for the red and near-infrared bands respectively. A threshold of approximately 0.5-0.65 was used to identify dirty/shady/bare ice, and one from 0.65-0.99 to identify snow-covered ice. Gridded files were then converted to polygons and additional manual editing was carried out to eliminate incorrectly classified regions.

Changes from Version 1.0 to Version 2.0:

Outlines of the glaciers of Mexico (16-02) were digitized by J.G. Cogley from maps in White (2002).

59 glaciers in east Africa (16-03) and seven in New Guinea (16-04) were added as nominal circles from WGI-XF.

Summary of quality controls conducted by E.S. Miles, University of British Columbia:

1. Version 1.0 RGI shapefile topology was corrected, splitting the complexes into glaciers (total of 14167 polygons).

2. Using the ice flowshed delineation script developed by C. Kienholz (UAF), the glacier polygons were divided into expected ice drainages. This processing preserved the original area of 5066.1 km^2 (measured in UTM 18S) and resulted in 16255 polygons.

3. All polygons smaller than 0.01 km^2 were then removed. A survey of these polygons showed that the vast majority were isolated and contained only 3 or 4 vertices. These small polygons (9869 in number) encompassed a total area of 20.8 km^2, again measured in UTM 18S.

4. The remaining 6386 polygons were individually inspected in ArcGIS with a standard ESRI satellite image basemap to remove gross inaccuracies.

    4.1. Due to difficulties in obtaining minimum-snow satellite imagery for the NDSI calculation used to create the initial dataset, there was significant snow contamination in the glacier dataset. The most obvious problems occurred in the severely arid regions of southern Peru and northern Chile, although problems were also evident in the temperate zones.

    4.2. Each polygon was inspected with consideration for the basemap satellite imagery, with scale fixed at 1:50,000 unless specific outlines warranted further inspection.

        4.2.1. Glacier outlines which were snow-covered or obscured by clouds in the basemap imagery were preserved as-is.

        4.2.2. Many glacier outlines encompassed both snow and rock (or vegetation, etc). If the snow portion was substantial (over a third or distributed over the entire outline), the outline was left as-is. If snow encompassed a very small and concentrated portion of the polygon, the polygon was roughly trimmed to this extent.

        4.2.3. Only glaciers containing no snow cover, where a debris-covered glacier was also implausible, were removed in their entirety.

    4.3. The resulting dataset included 4382 glacier outlines and 4088.2 km^2.

5. This inspection revealed an odd spatial shift for all polygons in a contiguous region between approximately Huaraz, Peru, and Conchucon, Peru. The features did not properly align with mountains evident in the ArcMap satellite imagery or in Google Earth. Most of the features appeared to be shifted by approximately 1.2km north of the mountains that they matched, and a zone near Huaraz show duplicated features in the outlines – one set of glaciers mapping correctly over the mountains with a matching set of features located about 1.2 km to the north. Probably due to an incorrect spatial representation of one of the source images used in the original glacier demarcation, the misregistration would be problematic for modelling.

     5.1. All glacier outlines within this region were extracted from the entire dataset (and deleted from the original). Individually, each glacier complex was uniformly shifted approximately 1.2km south, then adjusted to provide the best fit with topography and the satellite imagery backdrop. Since the required transformation was not quite linear (more shift was required for the northernmost outlines) it is likely that the source image had some minor distortion associated with the misregistration.

     5.2. The duplicate features were then manually trimmed (coarsely) according to a combination of the two outlines available in conjunction with the satellite image backdrop.

     5.3. After a satisfactory shift had been imposed, the individual glacier outlines were merged to a single polygon, and re-run through C. Kienholz's ice flowshed delineation script, such that the outlines would represent ice divides according to the correct topography.

     5.4. The corrected outlines were then merged back into the larger dataset and seams were trimmed where the polygons intersected.

6. The resulting dataset contains a total of 4373 outlines and covers an area of 4057.1 km^2.

7. Inspection of all polygon suggests that a more rigorous examination and delineation of each glacier would result in a further area reduction of up to 20%. Many outlines extend well beyond the terminus implied by the available satellite imagery, but the objective was primarily to remove the outlines that obviously did not represent glaciers at all.

Changes made from Version 2.0 to 3.0:
Some outlines in northern Chile were improved.

Changes made from Version 3.0 to 3.2:
Outlines of the glaciers of Mexico were replaced with outlines provided by E. Burgess, and the nominal glaciers of east Africa and New Guinea were replace with outlines provided by N.J. Cullen and A. Klein respectively. Note that several glacier complexes still exist in southern Peru and western Bolivia
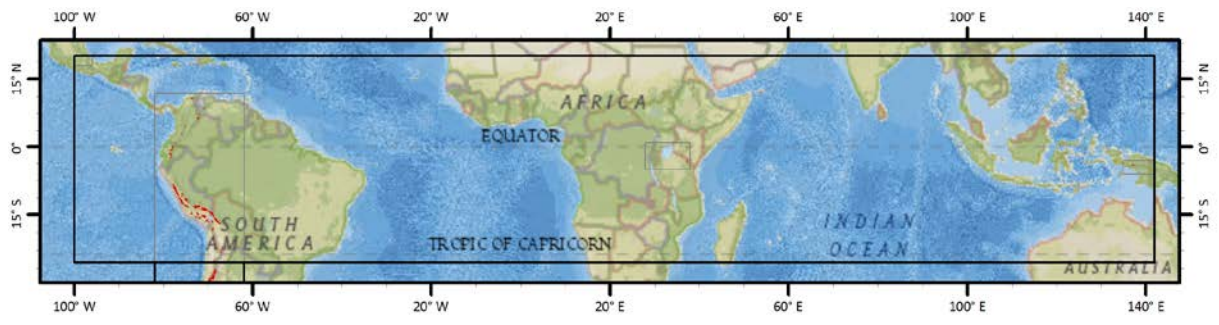
REGION 17: Southern Andes

Contributor	Institution	Project/Funding
Sharp, M.		
Wyatt, F.	University of Alberta, Canada	
Miles, E.	University of British Columbia, Canada	
De Angelis, H.	Stockholm University, Sweden	

Shapefiles were created from late summer, cloud free Landsat 7 ETM+ imagery acquired prior to the 2003 SLC failure. To identify glacier surfaces, a normalized difference snow index (NDSI) was calculated using bands 5 and 2 for the red and near-infrared bands respectively. A threshold of approximately 0.5-0.65 was used to identify dirty/shady/bare ice, and one from 0.65-0.99 to identify snow-covered ice. Gridded files were then converted to polygons and additional manual editing was carried out to eliminate incorrectly classified regions.

Shapefiles for the South Patagonian Icefield were provided by H. De Angelis (De Angelis, 2013).

Changes from Version 1.0 to Version 2.0:
Summary of quality controls conducted by E.S. Miles, University of British Columbia:
1. The original RGI shapefile's topology was corrected, splitting complexes into individual glaciers (total of 42,397 polygons covering 33786 km^2).

2. All polygons smaller than 0.01 km^2 were then removed. A survey of these polygons showed that (as in the Low-latitude Andes) the vast majority were isolated and contained only 3 or 4 vertices. These small polygons (26,396 in number) encompassed a total area of 59.23 km^2.
    2.1 The remaining 16,001 polygons were individually inspected in ArcGIS and compared to a standard ESRI satellite image basemap and a Bing Maps satellite basemap to remove gross inaccuracies. The Bing basemap was used primarily for areas where the ESRI image included substantial cloud cover. The two basemaps were qualitatively compared in cloud-free regions and the agreement was deemed satisfactory for the removal of blatantly erroneous data. For highly ambiguous zones, Google Earth was utilized as a third image and rough terrain dataset to help interpret the satellite images and glacier outlines.
    2.2 Due to difficulties in obtaining minimum-snow satellite imagery for the NDSI calculation used to create the initial dataset, there was significant snow contamination in the glacier dataset. This problem was most evident in southern Patagonia. Outlines in the Cordillera Darwin and the ranges east of the Icefields often reprezented snowlines rather than glacier outlines. Additionally, debris-covered glaciers and water-terminating glacial tongues posed significant problems for the NDSI algorithm. Finally, the utilization of Landsat-7 data inappropriately blended with Landsat-5 data led to substantial stripe patterns in some areas (different sampling dates resulted in a changed snowline between the striped L7 data and the solid L5 data).
    2.3 Each polygon was inspected with consideration for the basemap satellite imagery, with scale fixed at 1:60,000 unless specific outlines warranted further inspection.
        2.3.1 Glacier outlines which were snow-covered or obscured by clouds in all the basemap imagery were preserved as-is.
        2.3.2 Many glacier outlines encompassed both snow and rock (or vegetation, etc). If the snow portion was substantial (over a third or distributed over the entire outline), the outline was left as-is. If snow encompassed a very small and concentrated portion of the polygon, the polygon was roughly trimmed to this extent.
        2.3.3 Striping due to L5/L7 blending was edited where possible.

2.3.4 Many glacier outlines included peripheral zones that were implausible as connected zones of deforming ice, but realistically could include glacierets or other perennial ice cover. These zones were eliminated where possible, but were often left in the dataset.

2.3.5 Only glaciers where there was no snow cover and a debris-covered glacier was also implausible (lakes, vegetated slopes, snow-banked streams, etc.) were removed in their entirety.

2.3.6 Water-terminating glacier tongues were often enlarged to cover the extent shown in the satellite imagery. Debris exposed as the tongue melts seemed to frustrate the algorithm. The same problem arose with larger land-terminating glaciers whose tongues had accumulated significant debris.

2.3.7 Debris-covered glaciers were in some cases omitted in their entirety by the dataset. About 20-25 rough outlines of such glaciers were added, based on inspection of the three imagery datasets. Most were between 33.5 and 34.5 degrees South.

2.4 The resulting dataset included 14,014 glacier outlines.

3. The next step was to incorporate the glacier outlines for the Lagos region of Chile and Argentina, developed by F. Paul.

3.1 The extent of the source scenes was not perfectly clear, but F. Paul's dataset was assumed to cover region 17 in its entirety.

3.2 At the southern margin of this dataset, two glacier outlines had straight-line southern edges. They were assumed to be outlines falling on the satellite image's edge, and corresponded directly to RGI outlines that continued further south. These overlapping outlines were combined.

4. The combined dataset (edited RGI and F. Paul's outlines) was then processed with C. Kienholz's flowshed delineation algorithm.

5. The next step was to incorporate H. De Angelis' outlines for the South Patagonian Icefield.

5.1 All outlines that intersected the prior-version South Patagonian Icefield polygon (which blended into adjacent ranges due to snowline outlines) were extracted from the recently-edited dataset.

5.2 These outlines were then intersected with the De Angelis outlines, creating a combined dataset containing outlines split by flowsheds. These polygons were examined individually with respect to the same basemaps identified above.

5.2.1 De Angelis polygons were left as-is.

5.2.2 Polygons which appeared separated from the icefield were left as-is.

5.2.3 Exception: Sliver polygons removed from the icefield were removed when it was clear that editing had not produced a realistic flowshed.

5.2.4 Polygons adjacent to the icefield were included when the appearance of the basemap suggested an independent flowshed.

5.2.5 Polygons adjacent to the icefield were sometimes thin slivers (the recently-edited edited extent differed from the De Angelis extent), which were removed.

5.3 This dataset was then merged with the F. Paul and edited RGI outlines described above.

6. The final dataset (attached) contains 17,438 glacier outlines, covering a total area of 32,558 km2.

6.1 While the Southern Andes only exhibited a change of $1000 km^2$ of coverage as the result of this editing, the improvements were much more extensive than for the Low-latitude Andes.

6.2 Substantial reductions in area due to the elimination of false-positive area (lakes, snow, or vegetation cover included in glacier outlines) were largely offset by inclusion of false-negative area (debris-covered glaciers and water-terminating tongues). Via intermediate datasets it can be estimated that more than $2000 km^2$ of false-positive area were eliminated before the inclusion of $1000 km^2$ of false-negative area.

6.3 Where they were possible, eliminations of area led to much more realistic glacier outlines, rather than a fractured landscape. There are still substantial gains to be made in this realm, but those gains would require much more extensive efforts.

6.4 An estimated 5% error by area remains in the dataset, mostly as glacier-peripheral snow and transient ice, which is clearly evident in examination of the outlines. Since one connected ice mass (the North Patagonian Icefield) contains ~50% of the region's ice area, peripheral areas are minor on a percent-areal basis, but may amount to hundreds of km^2.

6.5 This dataset is assessed on the whole as yielding a conservative area estimate, having accounted for nearly all of the false-negative zones.

Changes from Version 2.0 to 3.2:
Substantial revisions were made by N. Mölg in central Chile and in the mountains surrounding the North and South Patagonian Ice Fields.
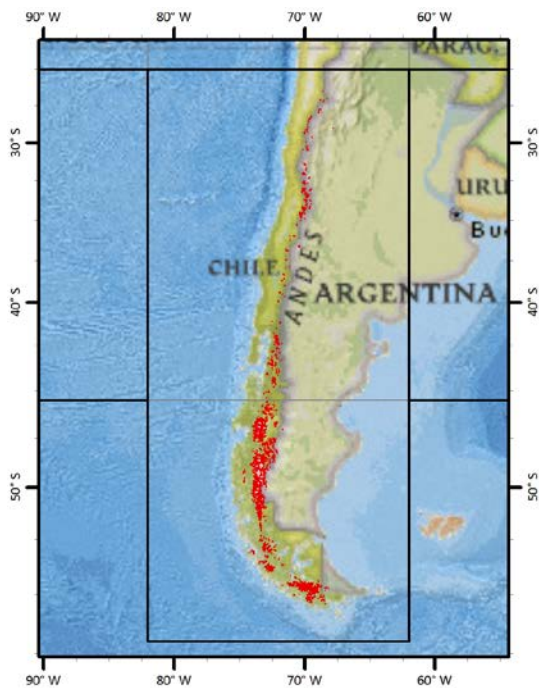
REGION 18: New Zealand

Contributor	Institution	Project/Funding
Chinn, T.	Canterbury University, NZ	

New Zealand outlines are derived from 1978 aerial imagery at a scale of 1:150,000 as used for the NZ Topo50 maps (Chinn, 2001). The shapefile can be downloaded from:
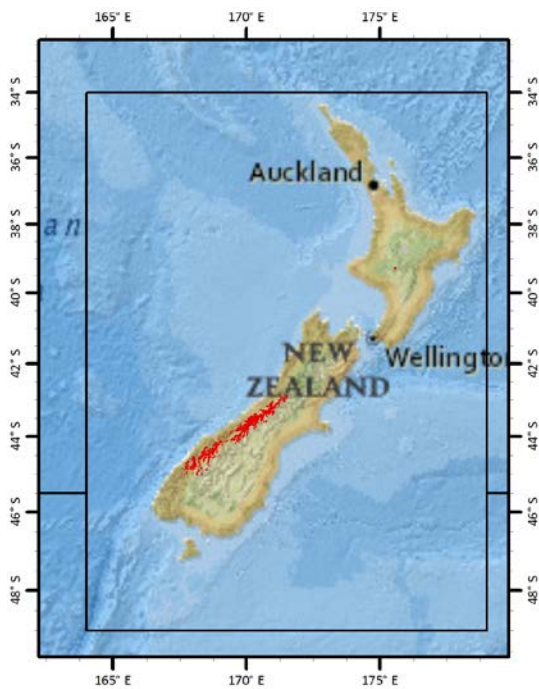
http://data.linz.govt.nz/#/layer/287-nz-mainland-ice-polygons-topo-150k/

Changes from Version 1.0 to Version 2.0:
No changes were made.

Changes from Version 2.0 to Version 3.0:
Glaciers were delineated from glacier complexes.

No changes were made from Version 3.0 to 3.2

REGION 19: Antarctic and Subantarctic

Contributor	Institution	Project/Funding
Bliss, A.	University of Alaska, Fairbanks, USA	
Hock, R.		
LeBris , R.	CNRS-OMP-LEGOS, France	
Berthier, E.		
Cogley, G.	Trent University, Canada	

Outlines of glacier complexes on islands peripheral to the mainland of Antarctica were obtained from the Antarctic Digital Database (ADD Consortium, 2000). A. Bliss manually classified the ADD's "land" polygons into continent, ice rise, ice cap, and glacier-complex polygons. Ice rises, and ice bodies on the continental mainland, are not included in this inventory. The classification was based on the surface morphology and surface flow velocities observed in data from Landsat, RADARSAT Antarctic Mapping Project DEM, and MEaSUREs InSAR-Based Antarctic Velocity Map. For islands with prominent nunataks, glacier complexes were subdivided into individual glaciers following Kienholz et al. (2013). More details on the processing of these outlines are given by Bliss et al. (2012).

Outlines of glaciers on the Subantarctic islands were obtained by G. Cogley from various sources including satellite imagery and maps (Cogley et al., 2013). For King George Island in the South Shetland Islands, outlines were downloaded from KGIS, the King George Island Geographic Information System, a now defunct web site created by F. Rau and S. Vogt, University of Freiburg. Separate outlines of "glacier basins" and ice-free areas were harmonized and merged to form glacier outlines containing nunataks. For Kerguelen, outlines are from Berthier et al. (2009). Outlines of South Georgia glaciers have been mapped by F. Paul from a Landsat ETM+ scene from 2003 using a band 3/5 ratio and manual corrections for icebergs and water (removed), and debris-cover (added); some regions covered by seasonal snow might be included.

Changes from Version 1.0 to Version 2.0:
The ice cover of Peter the First Island in the Bellingshausen Sea was taken from the ADD in version 1.0. In version 2.0 it is replaced by the outlines of 26 glaciers from an inventory by J.G. Cogley (Cogley et al., 2013).

Changes from Version 2.0 to Version 3.0:
The *TerminusType* digit of the *GlacType* attribute was coded following Paul et al. (2009) with the addition of code 5, representing shelf-terminating glaciers. Classification was done visually using imagery from a variety of sources. In a few instances, more than one terminus type applied to a particular glacier. Each such glacier was assigned the digit representing the longest part of its perimeter.
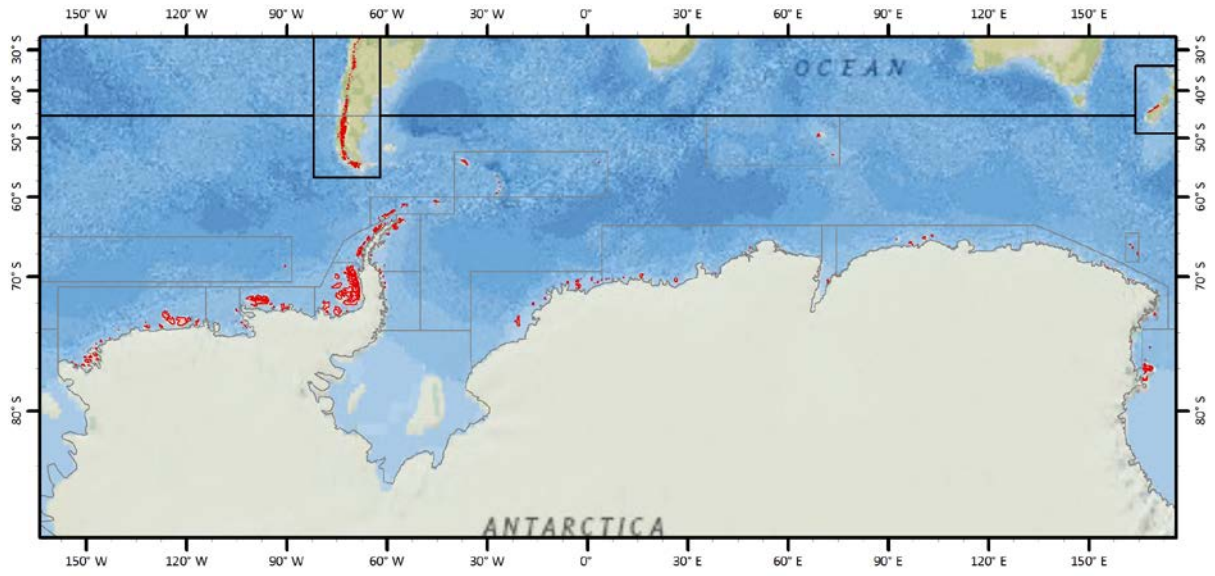
REFERENCES

ADD Consortium (2000), *Antarctic Digital Database, Version 3.0, Database, Manual and Bibliography*. Scientific Committee on Antarctic Research, Cambridge. 93p and digital data (version 4.1; http://www.add.scar.org/add_main.html).

Andreassen, L.M., F. Paul, A. Kääb, and J.E. Hausberg (2008), Landsat-derived glacier inventory for Jotunheimen, Norway, and deduced glacier changes since the 1930s, *The Cryosphere*, 2, 131-145.

Beedle, M., M. Dyurgerov, W. Tangborn, S. Khalsa, C. Helm, B. Raup, R. Armstrong, and R. Barry (2008), Improving estimation of glacier volume change: a GLIMS case study of Bering Glacier System, Alaska, *The Cryosphere*, 2, 33-51.

Berthier, E., R. Le Bris, L. Mabileau, L. Testut, and F. Rémy (2009), Ice wastage on the Kerguelen Islands(49S, 69E) between 1963 and 2006, *Journal of Geophysical Research*, 114 (F3), doi:10.1029/2008JF001192.

Berthier, E., E. Schiefer, G. Clarke, B. Menounos, and F. Rémy (2010), Contribution of alaskan glaciers to sea level rise derived from satellite imagery, *Nature Geoscience*, 3, 92-95, doi:10.1038/NGEO737.

Bliss, A., R. Hock and J.G. Cogley, 2013, A new inventory of mountain glaciers and ice caps for the Antarctic periphery, *Annals of Glaciology*, 54(63), doi:10.3189/2013AoG63A377.

Bolch, T. (2007), Climate change and glacier retreat in northern Tien Shan (Kazakhstan/Kyrgyzstan) using remote sensing data, *Global and Planetary Change, 56,* 1–12.

Bolch, T., B. Menounos, and R.D. Wheate (2010a), Landsat-based inventory of glaciers in western Canada, 1985 - 2005, *Remote Sensing of Environment, 114*(1), 127–137.

Bolch, T., T. Yao, S. Kang, M.F. Buchroithner, D. Scherer, F. Maussion, E. Huintjes, and C. Schneider (2010b), A glacier inventory for the western Nyainqentanglha Range and Nam Co Basin, Tibet, and glacier changes 1976-2009, *The Cryosphere, 4*, 419–433.

Cogley, J.G., 2009, A more complete version of the World Glacier Inventory, *Annals of Glaciology*, **50**(53), 32-38.

Cogley, J.G., E. Berthier and S. Donoghue, 2013, Glaciers of the Subantarctic islands, in Kargel, J.S., M.P. Bishop, A. Kääb, B. Raup and G. Leonard, eds., *Global Land Ice Measurements from Space: Satellite Multispectral Imaging of Glaciers*, Praxis-Springer, in press.

Chinn, T.J. (2001), Distribution of the glacial water resources of New Zealand, *Journal of Hydrology*, 40 (2), 139-187.

Citterio, M., F. Paul, A.P. Ahlstrøm, H.F. Jepsen, and A. Weidick (2009): Remote sensing of glacier change in West Greenland: accounting for the occurrence of surge-type glaciers, *Annals of Glaciology*, 50(53), 70-80.

Danko, D.M. (1992):   The digital chart of the world project, *Photogrammetric Engineering and Remote Sensing*, 58(8), 1125 – 1128.

De Angelis, H. (2013): Hypsometry and sensitivity of glaciers to changes in equilibrium line altitude: the case of the South Patagonian Icefield, *Journal of Glaciology*, submitted.

Frey, H., F. Paul, and T. Strozzi (in revision), Compilation of a glacier inventory for the western Himalayas from satellite data: Methods, challenges and results, *Remote Sensing of Environment*.

Gardner, A.S., G. Moholdt, J.G. Cogley, B. Wouters, A.A. Arendt, J. Wahr, E. Berthier, R. Hock, W.T. Pfeffer, G. Kaser, S.R.M. Ligtenberg, T. Bolch, M.J. Sharp, J.O. Hagen, M.R. van den Broeke and F. Paul (2013), A consensus estimate of glacier contributions to sea level rise: 2003 to 2009, *Science*, 340, 852-857.

Haeberli, W., M. Hoelzle, and S. Suter, eds., 1998, *Into the Second Century of World-Wide Glacier Monitoring – Prospects and Strategies*, UNESCO, Paris.

Hagen, J. O., O. Liestøl, E. Roland, and T. Jørgensen (1993), Glacier Atlas of Svalbard and Jan Mayen, *Norsk Polarinstitutt Meddelelser,* Nr. 129, Oslo.

Howat, I.M and A. Negrete (in prep.), A high-resolution ice mask for the Greenland Ice Sheet and peripheral glaciers and icecaps. http://bprc.osu.edu/GDG/icemask.php**.**

ICIMOD (2007), Inventory of glaciers, glacial lakes and identification of potential glacial lake outburst floods (GLOFs), Affected by Global Warming in the Mountains of Himalayan Region (Kathmandu, 2007).

ICIMOD (2011), Glacial lakes and glacial lake outburst floods in Nepal – additional material (ICIMOD, Kathmandu, 2011).

ICIMOD (2011), The Status of Glaciers in the Hindu Kush-Himalayan Region, Bajracharya, S., and B. Shrestha eds. International Centre for Integrated Mountain Development, Kathmandu, Nepal.

Kienholz, C., R. Hock and A. Arendt (2013), A new semi-automated approach for dividing glacier complexes into individual glaciers. *Journal of Glaciology,* 59(217), 925-937.

König, M., Nuth, C., Kohler, J., Moholdt, G., and Pettersen, R., (2013), A digital glacier database for Svalbard, in Kargel, J.S., M.P. Bishop, A. Kääb, B. Raup and G. Leonard, eds., *Global Land Ice Measurements from Space: Satellite Multispectral Imaging of Glaciers*, Praxis-Springer, in press.

Korona, J., Berthier, E., Bernard, M., Rèmy, F., and Thouvenot, E.: SPIRIT. SPOT 5 stereoscopic survey of Polar Ice (2009), Reference Images and Topographies during the fourth International Polar Year (2007-2009), *ISPRS Journal of Photogrammetry and Remote Sensing*, 64, 204-212.

Kutuzov, S., and M. Shahgedanova (2009), Glacier retreat and climatic variability in the eastern Terske-Alatoo, inner Tien Shan between the middle of the 19th century and beginning of the 21st century, *Global and Planetary Change,* 69(1-2), 59–70.

Kurter, A., 1991, Glaciers of Turkey, in Williams, R.S., Jr., and J.G. Ferrigno, eds., *Satellite Image Atlas of Glaciers of the World*, U.S. Geological Survey Professional Paper 1386-G, 1-30.

Le Bris, R., F. Paul, H. Frey, and T. Bolch (2011), A new satellite-derived glacier inventory for western Alaska, *Annals of Glaciology*, 52 (59), 135-143.

Liu, H., K. Jezek, B. Li, and Z. Zhao. (2001), *Radarsat Antarctic Mapping Project digital elevation model version 2*. Boulder, CO: National Snow and Ice Data Center. Digital media.

Moholdt, G., B. Wouters B., and A. Gardner (submitted), Recent mass changes of glaciers in the Russian High Arctic.

Moussavi, M.S., M.J. Valadan Zoej, F. Vaziri, M.R. Sahebi and Y. Rezaei, 2009, A new glacier inventory of Iran, *Annals of Glaciology*, 50(53), 93-103.

Nuth, C., J. Kohler, M. König, A. von Deschwanden, J. O. Hagen, A. Kääb, G. Moholdt1 and R. Pettersson (2013), Decadal changes from a multi-temporal glacier inventory of Svalbard. *The Cryosphere Discussions*, 7, 2489–2532, 2013.

Ohmura, A. (2009), Completing the World Glacier Inventory, *Annals of Glaciology,* 50(53), 144-148.

Paul, F. and A. Kääb (2005), Perspectives on the production of a glacier inventory from multispectral satellite data in the Canadian Arctic: Cumberland Peninsula, Baffin Island, *Annals of Glaciology*, 42, 59-66.

Paul, F. and L.M. Andreassen (2009), A new glacier inventory for the Svartisen region, Norway, from Landsat ETM+ data: challenges and change assessment, *Journal of Glaciology*, 55 (192), 607-618.

Paul, F. R.G. Barry, J.G. Cogley, H. Frey, W. Haeberli, A. Ohmura, C.S.L. Ommanney, B. Raup, A. Rivera, M. Zemp (2009). Recommendations for the compilation of glacier inventory data from digital sources. *Annals of Glaciology,* 50(53), 119-126.

Paul, F., L.M. Andreassen, and S.H. Winsvold (2011a), A new glacier inventory for the Jostedalsbreen region, Norway, from Landsat TM scenes of 2006 and changes since 1966, *Annals of Glaciology*, 52 (59), 153-162.

Paul, F., H. Frey, and R. Le Bris (2011b), A new glacier inventory for the European Alps from Landsat TM scenes of 2003: Challenges and results, *Annals of Glaciology*, 52 (59), 144-152.

Pfeffer, W.T., A.A. Arendt, A. Bliss, T. Bolch, J.G. Cogley, A.S. Gardner, J.-O. Hagen, R. Hock, G. Kaser, C. Kienholz, E.S. Miles, G. Moholdt, N. Mölg, F. Paul, V. Radić, P. Rastner, B.H. Raup, J. Rich, M.J. Sharp and the Randolph Consortium, 2013, The Randolph Glacier Inventory: a globally complete inventory of glaciers, *Journal of Geophysical Research*, submitted.

Raup, B., and S.J. Singh Khalsa, 2007, *GLIMS Analysis Tutorial*, http://glims.org. 8p.

Raup, B., H. Kieffer, T. Hare, and J. Kargel (2000), Generation of data acquisition requests for the ASTER satellite instrument for monitoring a globally distributed target: Glaciers, *IEEE Transactions on Geoscience and Remote Sensing,* 38, 1105–1112.

Raup, B., A. Kääb, J.S. Kargel, M. P. Bishop, G. Hamilton, E. Lee, F. Paul, F. Rau, D. Soltesz, S.J. Khalsa, et al. (2007), Remote sensing and GIS technology in the global land ice measurements from space (GLIMS) project, *Computers and Geosciences*, 33 (1), 104-125.

Rignot, E., J. Mouginot, and B. Scheuchl. (2011), Ice Flow of the Antarctic Ice Sheet, *Science*, 333(6048), 1427-1430. doi 10.1126/science.1208336.

Sarıkaya, M.A., and A.E. Tekeli, (2013), Satellite inventory of glaciers in Turkey, in Kargel, J.S., M.P. Bishop, A. Kääb, B. Raup and G. Leonard, eds., *Global Land Ice Measurements from Space: Satellite Multispectral Imaging of Glaciers*, Praxis-Springer, in press.

Sedov, R.V., 1997, Ledniki Chukotki, *Materialy Glyatsiologicheskikh Issledovaniy*, **82**, 213-217.

Shi, Y., C. Liu, and E. Kang (2009), The Glacier Inventory of China, *Annals of Glaciology 50*(53), 1–4.

Shroder, J.F., Jr., and M.P. Bishop, 2010, Selected glaciers of Afghanistan, in Williams, R.S., Jr., and J.G. Ferrigno, eds., *Satellite Image Atlas of Glaciers of the World – Asia*, U.S. Geological Survey Professional Paper 1386-F, 167-199. U.S. Government Printing Office, Washington, D.C.

Svoboda, F. and F. Paul (2009), A new glacier inventory on southern Baffin Island, Canada, from ASTER data: I. Applied methods, challenges and solutions, *Annals of Glaciology*, 50 (53), 11-21.

WGMS (1989): World glacier inventory - Status 1988. Haeberli, W., Bösch, H., Scherler, K., Østrem, G. and Wallén, C. C. (eds.), IAHS (ICSI) / UNEP / UNESCO, World Glacier Monitoring Service, Zurich, Switzerland: 458 pp.

White, S.E., 2002, Glaciers of Mexico, in Williams, R.S., Jr., and J.G. Ferrigno, eds., *Satellite Image Atlas of Glaciers of the World – North America*. U.S. Geological Survey Professional Paper 1386-J, 383-405. U.S. Government Printing Office, Washington, D.C.